Mechanisms of Development 155 (2019) 1–7

Contents lists available at ScienceDirect

Mechanisms of Development

journal homepage: www.elsevier.com/locate/mod

Cog4 is required for protrusion and extension of the epithelium in the developing semicircular canals

Aurélie Clément, Bernardo Blanco-Sánchez, Judy L. Peirce, Monte Westerfield*

Institute of Neuroscience, University of Oregon, Eugene, OR 97403, USA

ARTICLE INFO

Keywords:
Cog4
Pillar
Semicircular canal
Inner ear
Zebrafish

ABSTRACT

The semicircular canals in the inner ear sense angular acceleration. In zebrafish, the semicircular canals develop from epithelial projections that grow toward each other and fuse to form pillars. The growth of the epithelial projections is driven by the production and secretion of extracellular matrix components by the epithelium. The conserved oligomeric Golgi 4 protein, Cog4, functions in retrograde vesicle transport within the Golgi and mutations can lead to sensory neural hearing loss. In zebrafish *cog4* mutants, the inner ear is smaller and the number of hair cells is reduced. Here, we show that formation of the pillars is delayed and that secretion of extracellular matrix components (ECM) is impaired in *cog4*$^{-/-}$ mutants. These results show that Cog4 is required for secretion of ECM molecules essential to drive the growth of the epithelial projections and thus regulates morphogenesis of the semicircular canals.

1. Introduction

The inner ear is composed of the cochlea, for auditory sensation, and the vestibular apparatus essential for balance. In the vestibular apparatus, the vestibule and the semicircular canals detect linear and angular acceleration, respectively. The size and formation of semicircular canals differ among species (Alsina and Whitfield, 2017). In zebrafish, formation of the semicircular canals starts with epithelial projections of the otic vesicle that extend toward each other (Haddon and Lewis, 1996; Waterman and Bell, 1984). Opposite projections ultimately contact one another and fuse to form the pillars (Haddon and Lewis, 1996; Waterman and Bell, 1984) that later differentiate into semicircular canals.

In *Xenopus laevis*, scanning electron microscopy and Alcian blue staining showed that the epithelial projections are filled with extracellular matrix (ECM) and that the ECM drives their growth (Haddon and Lewis, 1991). Injection of hyaluronidase into the epithelial protrusions led to their collapse, indicating that hyaluronan is a major component of the ECM (Haddon and Lewis, 1991). In addition, Geng and colleagues showed that the epithelial projections express several markers of the ECM during their growth, such as hyaluronan, chondroitin sulfate proteoglycan, and collagen type II (Geng et al., 2013).

A critical step in making the ECM is secretion of its components. The Conserved oligomeric Golgi (COG) complex is composed of eight proteins, COG1-8, distributed between two lobes, A and B. The COG complex functions in retrograde vesicle transport within the Golgi, particularly vesicle tethering (Miller and Ungar, 2012). Physiologically, the COG proteins participate in sorting glycosylation enzymes to maintain glycosylation homeostasis (Miller and Ungar, 2012). Thus, defects in COG proteins lead to aberrant glycoconjugate synthesis, protein sorting, and protein secretion. The COG4 protein is a subunit of lobe A. In humans, *COG4* mutations lead to congenital disorders of glycosylation type IIJ. Patients affected with this disease present with a range of symptoms including dysmorphia, microcephaly, developmental delay, hypotonia, seizures, failure to thrive, coagulopathy, liver cirrhosis, and nystagmus (Ng et al., 2011; Reynders et al., 2009; Richardson et al., 2009). Recently, a mutation in COG4 was associated with Saul-Wilson syndrome, a rare disease characterized by dysmorphia and developmental delay (Ferreira et al., in press). Some patients with this mutation also display sensorineural hearing loss. In zebrafish mutants for *cog4*, we found phenotypes similar to the symptoms of human Saul-Wilson syndrome. *cog4*$^{-/-}$ mutants are shorter and display smaller jaws, due to improper stacking of chondrocytes, stubby pectoral fins, and smaller eyes and ears (Ferreira et al., in press).

Here, we investigated the mechanism that gives rise to the inner ear phenotype in zebrafish *cog4* mutants. We found that the semicircular canals do not develop correctly in *cog4*$^{-/-}$ mutants. Extension of the epithelial projections that form the pillars is delayed. We show that this delay is due to defective secretion of ECM components.

* Corresponding author.
E-mail address: monte@uoneuro.uoregon.edu (M. Westerfield).

https://doi.org/10.1016/j.mod.2018.09.003
Received 28 June 2018; Received in revised form 6 September 2018; Accepted 22 September 2018
Available online 01 October 2018
0925-4773/ © 2018 Elsevier B.V. All rights reserved.

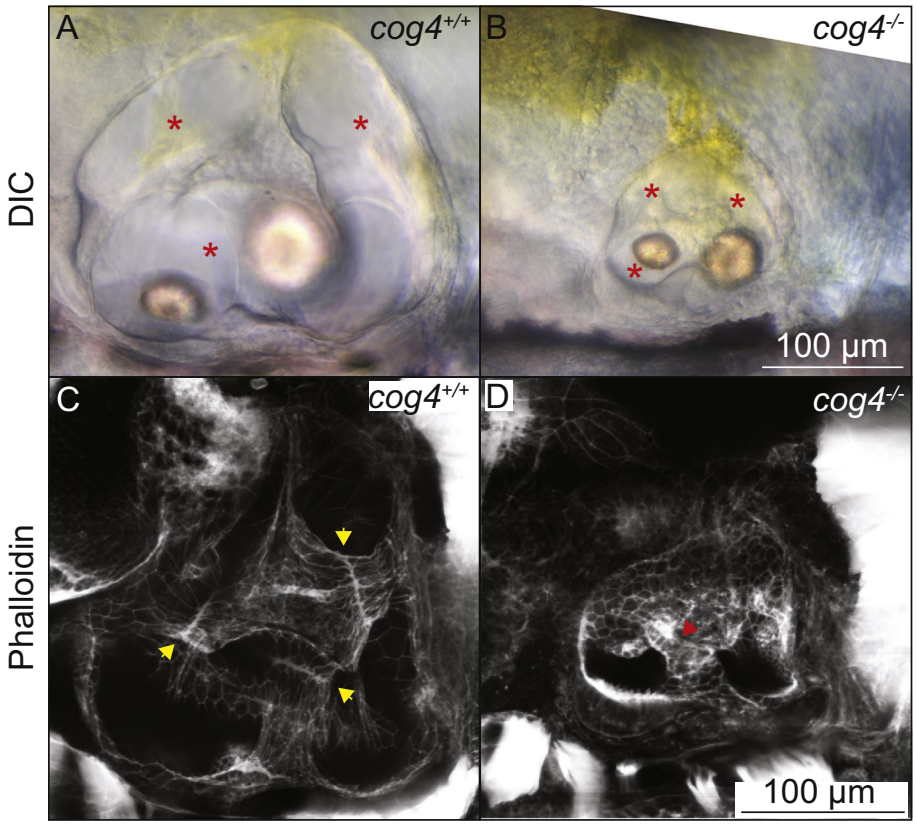

Fig. 1. The pillars do not form properly in *cog4*$^{-/-}$ mutants. Live images of the inner ear of *cog4*$^{+/+}$ sibling (A, n = 34 larvae) and *cog4*$^{-/-}$ mutant larvae (B, n = 15 larvae). Red stars indicate the semicircular canals. Phalloidin staining of the inner ear of *cog4*$^{+/+}$ sibling (C, n = 24 larvae) and *cog4*$^{-/-}$ mutant larvae (D, n = 25 larvae). Yellow arrowheads indicate the fusion plates that form in 100% (24 out of 24) of wild-type siblings (C). Red arrowhead points to the malformed pillar. One or more malformed pillars are observed in 84% (21 out of 25) of homozygous mutant larvae (D). Anterior to the left and dorsal to the top. 5 dpf.

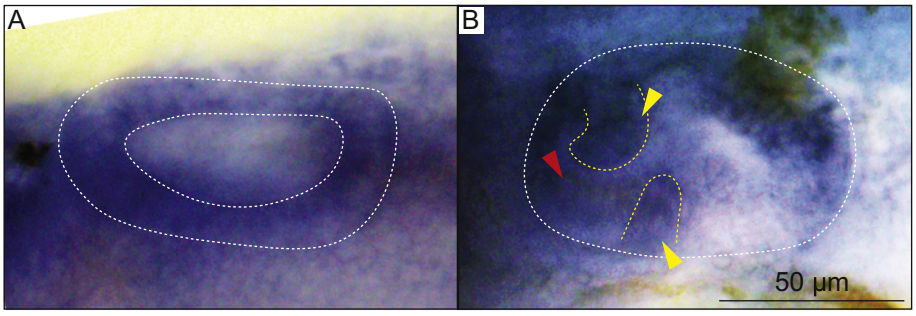

Fig. 2. *cog4* is differentially expressed during inner ear morphogenesis. *In situ* hybridization of *cog4* in the ear at 28 hpf (A, n = 18 embryos), and 52 hpf (B, n = 18 larvae). Dorsal view, anterior to the left (A). Lateral view, anterior to the left (B). Yellow arrowheads indicate the anterior and ventral projections. Red arrowhead indicates the hair cells of the anterior macula (B). The inner ear is outlined in white (A, B) and the epithelial projections in yellow (B).

2. Experimental procedures

2.1. Zebrafish maintenance and staging

Wild-type ABCxTu and heterozygous mutant *cog4*$^{b1312/+}$ (Ferreira et al., in press) adult zebrafish were maintained as previously described (Westerfield, 2007). The *cog4*^{b1312} allele is a 13 bp deletion in exon 12 of *cog4*. The mutation introduces a frameshift followed by an early stop codon (Ferreira et al., in press). Complementation tests with another allele of *cog4* (Ferreira et al., in press) indicate that this allele is a null allele. Embryos and larvae were staged according to the standard staging series (Kimmel et al., 1995). Siblings are defined as a mix of homozygous WT and heterozygous mutants generated by incrosses of heterozygous mutant adults. All experimental procedures were approved by the local IACUC.

2.2. In situ hybridization and histology

The procedure followed the previously published protocol (Thisse and Thisse, 2008). Larvae were hybridized with a digoxigenin labeled RNA probe spanning a 736 bp coding sequence between exons 3 and 8 of *cog4* (Ferreira et al., in press). Stained larvae were embedded in 1% agarose, 0.5% agar, and 5% sucrose medium and 16 µm cryosections were cut.

2.3. Immunolabeling, phalloidin staining, Alcian blue staining

Wholemount larvae were stained following our previously published protocol (Blanco-Sanchez et al., 2014) with minor modifications. 52 h post-fertilization (hpf) and 5 days post-fertilization (dpf) larvae were fixed in BT fix overnight and permeabilized with proteinase K (10 µg/ml) for 30 min or 1 h, respectively. Primary antibodies were mouse anti-Collagen type II (Developmental Studies Hybridoma Bank, II-II6B3; 1:200). Secondary antibodies were goat anti-mouse Alexa-Fluor-568-conjugated (Vector Laboratories, 1:200). Phalloidin staining was performed as previously described (Blanco-Sanchez et al., 2014). Alcian blue staining was performed as previously described (Walker and Kimmel, 2007).

2.4. Drug treatment

Brefeldin A (Sigma; BFA) was suspended in ethanol at a stock

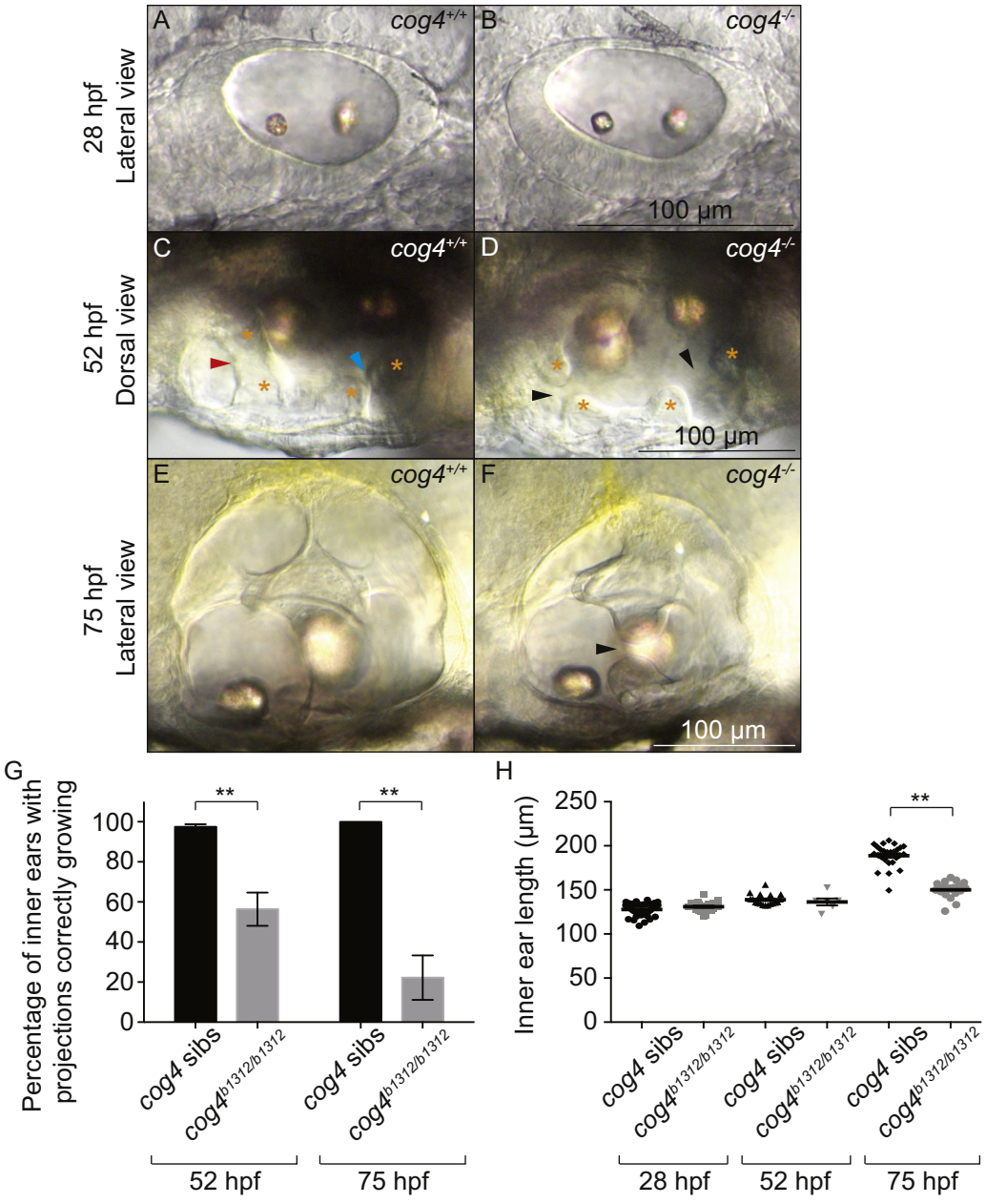

Fig. 3. Formation of the epithelial projections is delayed in *cog4*$^{-/-}$ mutants. Live images of the inner ear from *cog4*$^{+/+}$ sibling (A, n = 49 embryos; C, n = 57 larvae; E, n = 26 larvae) and *cog4*$^{-/-}$ mutant larvae (B, n = 21 embryos; D, n = 22 larvae; F, n = 18 larvae) at 28 hpf (A, B), 52 hpf (C, D) and 75 hpf (E, F). Orange stars indicate the anterior and posterior projections and bulges (C, D). The red and blue arrowheads indicate the anterior and forming posterior pillar, respectively (C). Black arrowheads point to the gaps between the anterior and forming posterior projections and bulges (D, F). Anterior to the left (A–F). Dorsal to the top (A, B, E, F). Medial to the top (C, D). Percentage of inner ears with projections growing correctly at 52 hpf and 75 hpf, in *cog4*$^{+/+}$ sibling (52 hpf, n = 114 inner ears; 75 hpf, n = 26 inner ears) and *cog4*$^{-/-}$ mutant larvae (52 hpf, n = 38 inner ears; 75 hpf, n = 18 inner ears) (G). Ear size at 28, 52 and 75 hpf in *cog4*$^{+/+}$ sibling (28 hpf, n = 49 embryos; 52 hpf, n = 18 larvae; 75 hpf, n = 26 larvae) and *cog4*$^{-/-}$ mutant larvae (28 hpf, n = 21 embryos; 52 hpf, n = 6 larvae; 75 hpf, n = 18 larvae) (H). Size was measured along the antero-posterior axis of the inner ear. Data are represented as mean ± SEM. **p < 0.01.

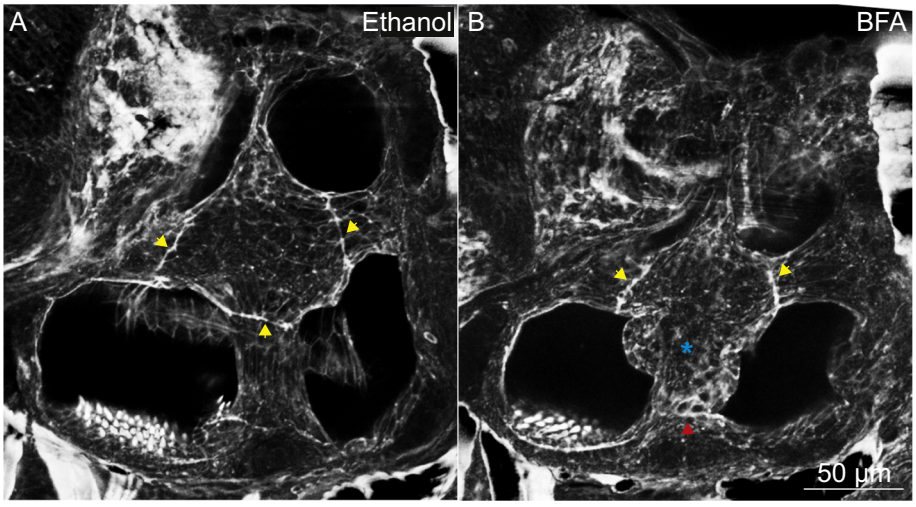

Fig. 4. The pillars do not form properly in larvae treated with BFA. Phalloidin staining of the inner ear in larvae treated with ethanol (A; control, n = 10 larvae) or BFA (B, n = 10 larvae). Yellow arrowheads indicate the fusion plates. Red arrowhead indicates an abnormal fusion plate. Blue star indicates the malformed pillar. Anterior to the left and dorsal to the top. 5 dpf.

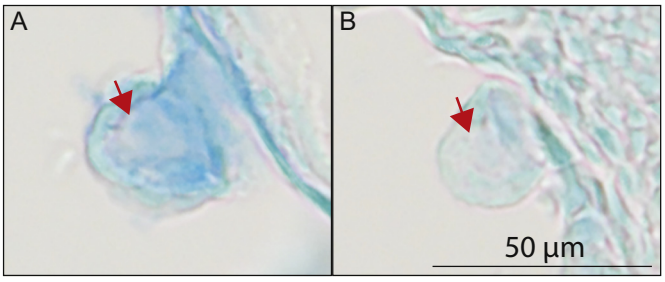

Fig. 5. The secretion of proteoglycans from the epithelial projections is reduced in *cog4*$^{-/-}$ mutants. Paraffin section of the inner ear posterior projection in *cog4*$^{+/+}$ (A, n = 6 larvae) and *cog4*$^{-/-}$ larvae (B, n = 7 larvae). Alcian blue staining was performed prior to sectioning. Red arrows indicate the projection core. Anterior to the left and dorsal to the top. 52 hpf.

concentration of 10 mg/ml, and stored at −20 °C. Wild-type larvae were incubated with BFA or ethanol as follows: 10 µg/ml of BFA (experimental condition) or an equal volume of ethanol (control condition) was added to the embryo medium from 2 dpf to 5 dpf, at which stage larvae were fixed.

2.5. Imaging

Differential interference contrast images of the inner ear and images of embryos/larvae stained by *in situ* hybridization and Alcian blue were acquired using a Zeiss Axioplan2 compound microscope. Images of immunolabeled larvae were acquired using a Zeiss LSM 5 confocal microscope. Images were analyzed using ImageJ.

All embryos and larvae treated, labeled, and/or stained were imaged and analyzed. For *in situ* hybridization experiments, all embryos and larvae were analyzed, and only two individuals were imaged per stage of interest.

3. Results

3.1. The pillars are misshaped in cog4$^{-/-}$ mutants

We previously found that the inner ear is smaller in 5 dpf *cog4*$^{-/-}$ mutant larvae, but that the three semicircular canals form (Fig. 1A, B) (Ferreira et al., in press). To understand the function of Cog4 in the inner ear, we examined the structure of the semicircular canals as they develop. Phalloidin staining in wild-type larvae at 5 dpf revealed a thin fusion plate where the epithelial projections have met and fused (Fig. 1C, yellow arrowheads). In *cog4*$^{-/-}$ mutant larvae, the fusion plates are not well defined (Fig. 1D, red arrowhead). This led us to the hypothesis that Cog4 is required for formation of the pillars.

To gain a better understanding of how Cog4 acts, we examined *cog4* expression. RT-PCR showed that *cog4* is maternally deposited and expressed at least through early larval stages (Supplemental Fig. S1). We also performed *in situ* hybridization at various stages during inner ear development. At 28 hpf, *cog4* was expressed ubiquitously and throughout the entire epithelium of the otic vesicle (Fig. 2A and Supplemental Fig. S2A). At 52 hpf, *cog4* was also expressed ubiquitously and more strongly in the epithelial projections and hair cells (Fig. 2B, yellow and red arrowheads, respectively, and Supplemental Fig. S2B). This spatiotemporal expression pattern suggests a role for Cog4 in morphogenesis of the semicircular canals. Supporting this, expression of *cog4* was previously observed in inner ear hair cells at 5 dpf (Ferreira et al., in press).

3.2. Cog4 is required for the growth of the epithelial projections

These results (Figs. 1 and 2) suggested that Cog4 is necessary for pillar formation. To determine the process affected by lack of Cog4, we analyzed the structure of the inner ear as it develops using live imaging techniques. After the otic vesicle cavitates at 17 hpf, it undergoes a dorsal thinning and ventral thickening of the epithelium (Lang et al., 2000; Ohta et al., 2010). Cells in the dorsolateral region will give rise to the semicircular canals. At 28 hpf, *cog4*$^{-/-}$ embryos had a properly shaped otic vesicle with a thin dorsal epithelium (Fig. 3A, B). This indicated that the precursors of the semicircular canals were present.

The first protrusions of epithelium that will give rise to the pillars appear between 42 and 48 hpf (Haddon and Lewis, 1996). The projections then grow and extend until they touch and fuse (Fig. 3C) (Haddon and Lewis, 1996). In *cog4*$^{-/-}$ mutant larvae, growth of the projections was delayed (Fig. 3D). In 42% (16 out of 38) of the inner ears analyzed in *cog4*$^{-/-}$ mutant larvae at 52 hpf, the projections still looked like early protrusions from the epithelium and had not grown enough to contact the opposite projections (Fig. 3D, black arrowheads and Fig. 3G).

In normal animals, the three pillars, anterior, posterior and horizontal, form by 72 hpf, and the three semicircular canals are defined (Fig. 3E) (Haddon and Lewis, 1996). In *cog4*$^{-/-}$ mutant larvae, the three pillars were not always formed even by 75 hpf (Fig. 3F). We found that only 22% (4 out of 18) of *cog4*$^{-/-}$ mutant inner ears had three fused pillars, in contrast to 100% (26 out of 26) of the inner ears analyzed in wild-type larvae (Fig. 3G). The 78% (14 out of 18) of remaining *cog4*$^{-/-}$ mutant inner ears had at least one unfused pillar (Fig. 3F, black arrowhead).

Our previous results show that at 5 dpf the three semicircular canals are present in the *cog4*$^{-/-}$ mutants (Fig. 1B, D), suggesting that the epithelial projections ultimately fuse. Fusion plates are determined by the presence of F-actin and indicate that the two cell populations have met. In *cog4* siblings, the fusion plates appear as a thin line. Interestingly in the *cog4*$^{-/-}$ mutants, the fusion plates are not well defined (Fig. 1C, D; arrowheads), suggesting that the projections have overgrown. Together, these data indicate that Cog4 is essential for proper growth and fusion of the epithelial projections of the otic vesicle.

Because the inner ear is smaller at 5 dpf in *cog4* mutants (Fig. 1) (Ferreira et al., in press), we measured its size along the antero-posterior axis at earlier developmental stages to assay when the defects can be visualized. No difference was observed at 28 hpf, nor at 52 hpf when the projection phenotype is observed (Fig. 3H). However, the inner ears were significantly smaller at 75 hpf.

To eliminate the possibility that the defect in semicircular canal morphogenesis is due to abnormal sensory tissue, we checked whether the cristae were forming or not. We found that the anterior, lateral and posterior cristae are all present at 5 dpf (Supplemental Fig. S3).

3.3. Inhibition of protein trafficking leads to misshaped pillars

To confirm that Cog4 function in protein trafficking is responsible for the otic phenotype observed in *cog4*$^{-/-}$ mutants, we used an inhibitor of protein trafficking, BFA, and analyzed the semicircular canals at 5 dpf. BFA prevents anterograde transport of secretory proteins from the ER to the Golgi, resulting in collapse of the Golgi (Klausner et al., 1992; Misumi et al., 1986; Pelham, 1991). In 100% (10 out of 10) control larvae treated with ethanol from 2 dpf to 5 dpf, the epithelial projections grew and fused to form the pillars normally, and the fusion plates resembled those found in untreated wild-type larvae (Fig. 4A, yellow arrowheads). In 100% (10 out of 10) larvae treated with BFA from 2 dpf to 5 dpf, however, the projections grow abnormally resulting in misshaped pillars, and the fusion plates are not always defined (Fig. 4B, blue star and red arrowhead, respectively), similar to *cog4*$^{-/-}$ mutant ears. In addition, and also similar to *cog4*$^{-/-}$ mutants, the inner ears were smaller in the BFA treated larvae (Fig. 4).

3.4. Secretion of ECM is disrupted in cog4$^{-/-}$ mutants

The core of each epithelial projection of the otic vesicle is filled with

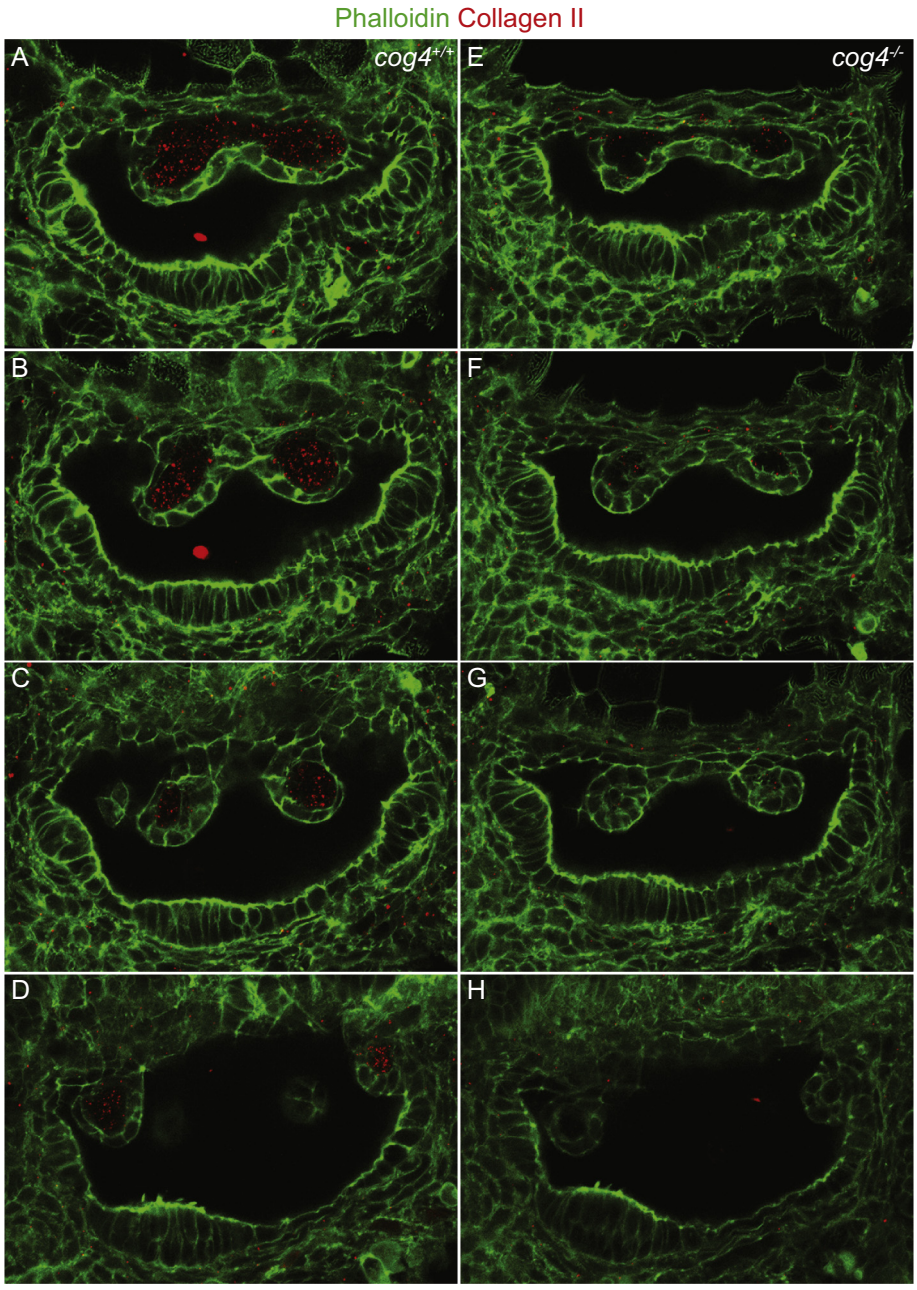

Fig. 6. The secretion of Collagen type II from the epithelial projections is reduced in *cog4*$^{-/-}$ mutants. Series of confocal sections through the inner ear of *cog4*$^{+/+}$ (A–D; n = 9 larvae) and *cog4*$^{-/-}$ larvae (E–H, n = 8 larvae). The most lateral section is at the top and most medial at the bottom. Anterior to the left and dorsal to the top. 52 hpf.

ECM components secreted by the cells of the epithelium (Haddon and Lewis, 1991). This ECM is known to drive the growth of each projection (Geng et al., 2013; Haddon and Lewis, 1991). We previously showed that secretion of ECM components by chondrocytes is severely decreased in *cog4*$^{-/-}$ mutants (Ferreira et al., in press). We thus examined whether secretion of ECM components is also affected in the epithelial projections of the inner ear. For this, we used Alcian blue staining at 2 dpf to analyze secretion of proteoglycans. In wild-type larvae, Alcian blue staining was strong in the projection core indicating that proteoglycans had been secreted (Fig. 5A and Supplemental Fig. S4A, B, F–H). In contrast, Alcian blue staining was weak in *cog4*$^{-/-}$ mutants, suggesting that the ECM core of the projections was deficient in proteoglycans (Fig. 5B and Supplemental Fig. S4C–E, I–K).

Collagen type II is an ECM component present in the projections and the pillars (Dale and Topczewski, 2011; Geng et al., 2013). Immunolabeling of Collagen type II at 52 hpf showed that this protein is abundantly secreted into the core of the projections of wild-type larvae (Fig. 6A–D). In *cog4*$^{-/-}$ mutants however, secretion of Collagen type II was highly diminished (Fig. 6E–H).

To learn whether secretion of Collagen type II later recovers in *cog4*$^{-/-}$ mutants, we examined 5 dpf animals. At this stage of development, Collagen type II is normally present in the semicircular canals (Geng et al., 2013). In wild-type larvae, we found Collagen type II in the pillars, the dorsolateral septum, and in the common crus (Supplemental Fig. S2A). Interestingly, the level of Collagen type II labeling in *cog4*$^{-/-}$ mutants was similar to their siblings in the pillars and common crus (Supplemental Fig. S2B, C). In addition, ectopic accumulation of this ECM component was observed in the lumen of the semicircular canals. This suggests that, at later stages, another trafficking pathway may compensate to some extent for the lack of Cog4 function.

Together, these data support the hypothesis that defective secretion of ECM components is responsible for abnormal growth of the epithelial projections of the inner ear in *cog4*$^{-/-}$ mutants.

4. Discussion

The semicircular canals of the inner ear are required for proper vestibular function. In zebrafish, the steps leading to formation of the semicircular canals are well understood (Alsina and Whitfield, 2017; Geng et al., 2013; Haddon and Lewis, 1996; Haddon and Lewis, 1991; Waterman and Bell, 1984). Specifically, secretion of ECM components by epithelial cells of the otic vesicle is essential for growth of the projections and formation of the pillars. We have previously shown in zebrafish and cell culture that Cog4 is required for protein trafficking at the Golgi and secretion of components of the ECM (Ferreira et al., in press). Here, we show that Cog4 dependent trafficking and secretion of ECM components are required for protrusion and extension of the epithelial projections of the inner ear.

In addition to the inner ear phenotype, *cog4*$^{-/-}$ mutant larvae are also shorter and exhibit smaller jaws and stubby pectoral fins (Ferreira et al., in press). A similar spectrum of phenotypes has been observed previously in a group of zebrafish mutants identified in a large-scale screen for craniofacial defects (Neuhauss et al., 1996). In that group, mutants are shorter, the pharyngeal skeleton is reduced, the pectoral fins are kinked and/or shorter, and the semicircular canals of the inner ear fail to form. Although all the affected genes have not yet been identified, a number of them are involved in trafficking. In *bulldog*, *crusher*, and *feelgood*, the mutated genes, *sec24d*, *sec23a*, and *creb3l2*, respectively, encode proteins of the COPII secretory pathway (Lang et al., 2006; Melville et al., 2011; Sarmah et al., 2010). In *jekyll* (*jek*) mutants, Alcian blue staining of head cartilage is very weak (Neuhauss et al., 1996), a phenotype that we also observed in *cog4* mutants (Ferreira et al., in press). *jek* mutants carry mutations in UDP-glucose dehydrogenase, an enzyme involved in synthesis of proteoglycans such as hyaluronan, a major ECM component of the inner ear epithelial projections (Busch-Nentwich et al., 2004; Haddon and Lewis, 1991; Walsh and Stainier, 2001).

Hyaluronan acts as a propellant for the epithelial protrusions of the inner ear by filling the pillar core. Similar to the head cartilage in *jek* and *cog4* mutants (Ferreira et al., in press; Neuhauss et al., 1996), Alcian blue staining of the pillar core is diminished after treatment by hyaluronidase (Haddon and Lewis, 1991). We observed a similar decrease of Alcian blue staining in the protrusions of *cog4* mutants. Our results thus indicate that Cog4 plays a crucial role in secretion of ECM components and that, in the inner ear, it may be required for secretion of hyaluronan.

In zebrafish, the semicircular canals form between 42 and 72 hpf, starting with protrusions from the otic epithelium between 42 hpf and 48 hpf (Haddon and Lewis, 1996; Waterman and Bell, 1984). At 52 hpf, *cog4* mutants present a significant delay in growth of the projections and reduced levels of Collagen type II in these structures. However, by 5 dpf, Collagen type II is present in the semicircular canals of *cog4* mutants, and the semicircular canals have formed. This suggests that Cog4 is specifically necessary in early morphogenesis of the inner ear semicircular canals.

The G-coupled receptor gene, *gpr126*, encodes a protein that regulates expression of several ECM genes in the semicircular canal projections (Geng et al., 2013). When this gene is mutated in the *lauscher* mutants, projections grow but fail to fuse to form the pillars (Geng et al., 2013; Whitfield et al., 1996). As a result, ears are swollen at 5 dpf. When ear projections from wild-type embryos are injected with hyaluronidase before fusion occurs, the projections do not grow and the ears are swollen (Geng et al., 2013). Despite the function of Cog4 in secretion of ECM components, defects in *cog4* mutants differ: the semicircular canals ultimately form and the ears do not appear swollen (Ferreira et al., in press and this paper). This weaker phenotype could be due to a narrower developmental time window during which Cog4 is required in the ear.

Zebrafish genetics has identified a set of genes required for formation of the semicircular canals, including several that function in formation of the ECM (Busch-Nentwich et al., 2004; Geng et al., 2013; Haddon and Lewis, 1991; Neuhauss et al., 1996; Rotllant et al., 2008). By identifying more components in this pathway, we will be able to dissect precisely the molecular and cellular mechanisms leading to proper morphogenesis of the semicircular canals, as well as what goes wrong in human disease.

Supplementary data to this article can be found online at https://doi.org/10.1016/j.mod.2018.09.003.

Acknowledgements

We thank Poh Kheng Loi for her technical assistance with histology. This work was supported by grants from the National Institutes of Health (HD22486, NS093793, DC010447).

Declaration of interests

The authors declare no competing interests.

References

Alsina, B., Whitfield, T.T., 2017. Sculpting the labyrinth: morphogenesis of the developing inner ear. Semin. Cell Dev. Biol. 65, 47–59.
Blanco-Sanchez, B., Clement, A., Fierro Jr., J., Washbourne, P., Westerfield, M., 2014. Complexes of usher proteins preassemble at the endoplasmic reticulum and are required for trafficking and ER homeostasis. Dis. Model. Mech. 7, 547–559.
Busch-Nentwich, E., Sollner, C., Roehl, H., Nicolson, T., 2004. The deafness gene dfna5 is crucial for ugdh expression and HA production in the developing ear in zebrafish. Development 131, 943–951.
Dale, R.M., Topczewski, J., 2011. Identification of an evolutionarily conserved regulatory element of the zebrafish col2a1a gene. Dev. Biol. 357, 518–531.
Ferreira, C.R., Xia, Z., Clément, A., Parry, D.A., Davids, M., Taylan, F., Sharma, P., Turgeon, C.T., Blanco-Sánchez, B., Ng, B.G., et al., 2018. A recurrent de novo heterozygous COG4 variant leads to Saul-Wilson syndrome, disruption of vesicular trafficking, abnormal Golgi structure and altered glycosylation of a secreted proteoglycan. Am. J. Hum. Genet (in press).
Geng, F.S., Abbas, L., Baxendale, S., Holdsworth, C.J., Swanson, A.G., Slanchev, K., Hammerschmidt, M., Topczewski, J., Whitfield, T.T., 2013. Semicircular canal morphogenesis in the zebrafish inner ear requires the function of gpr126 (lauscher), an adhesion class G protein-coupled receptor gene. Development 140, 4362–4374.
Haddon, C.M., Lewis, J.H., 1991. Hyaluronan as a propellant for epithelial movement: the development of semicircular canals in the inner ear of *Xenopus*. Development 112, 541–550.
Haddon, C., Lewis, J., 1996. Early ear development in the embryo of the zebrafish, *Danio rerio*. J. Comp. Neurol. 365, 113–128.
Kimmel, C.B., Ballard, W.W., Kimmel, S.R., Ullmann, B., Schilling, T.F., 1995. Stages of embryonic development of the zebrafish. Dev. Dyn. 203, 253–310.
Klausner, R.D., Donaldson, J.G., Lippincott-Schwartz, J., 1992. Brefeldin A: insights into the control of membrane traffic and organelle structure. J. Cell Biol. 116, 1071–1080.
Lang, H., Bever, M.M., Fekete, D.M., 2000. Cell proliferation and cell death in the developing chick inner ear: spatial and temporal patterns. J. Comp. Neurol. 417, 205–220.
Lang, M.R., Lapierre, L.A., Frotscher, M., Goldenring, J.R., Knapik, E.W., 2006. Secretory COPII coat component Sec23a is essential for craniofacial chondrocyte maturation. Nat. Genet. 38, 1198–1203.
Melville, D.B., Montero-Balaguer, M., Levic, D.S., Bradley, K., Smith, J.R., Hatzopoulos, A.K., Knapik, E.W., 2011. The feelgood mutation in zebrafish dysregulates COPII-dependent secretion of select extracellular matrix proteins in skeletal morphogenesis. Dis. Model. Mech. 4, 763–776.
Miller, V.J., Ungar, D., 2012. Re'COG'nition at the Golgi. Traffic 13, 891–897.
Misumi, Y., Misumi, Y., Miki, K., Takatsuki, A., Tamura, G., Ikehara, Y., 1986. Novel blockade by brefeldin A of intracellular transport of secretory proteins in cultured rat hepatocytes. J. Biol. Chem. 261, 11398–11403.
Neuhauss, S.C., Solnica-Krezel, L., Schier, A.F., Zwartkruis, F., Stemple, D.L., Malicki, J., Abdelilah, S., Stainier, D.Y., Driever, W., 1996. Mutations affecting craniofacial development in zebrafish. Development 123, 357–367.
Ng, B.G., Sharma, V., Sun, L., Loh, E., Hong, W., Tay, S.K., Freeze, H.H., 2011. Identification of the first COG-CDG patient of Indian origin. Mol. Genet. Metab. 102, 364–367.
Ohta, S., Mansour, S.L., Schoenwolf, G.C., 2010. BMP/SMAD signaling regulates the cell behaviors that drive the initial dorsal-specific regional morphogenesis of the otocyst. Dev. Biol. 347, 369–381.
Pelham, H.R., 1991. Multiple targets for brefeldin A. Cell 67, 449–451.
Reynders, E., Foulquier, F., Leao Teles, E., Quelhas, D., Morelle, W., Rabouille, C.,

Annaert, W., Matthijs, G., 2009. Golgi function and dysfunction in the first COG4-deficient CDG type II patient. Hum. Mol. Genet. 18, 3244–3256.
Richardson, B.C., Smith, R.D., Ungar, D., Nakamura, A., Jeffrey, P.D., Lupashin, V.V., Hughson, F.M., 2009. Structural basis for a human glycosylation disorder caused by mutation of the COG4 gene. Proc. Natl. Acad. Sci. U. S. A. 106, 13329–13334.
Rotllant, J., Liu, D., Yan, Y.L., Postlethwait, J.H., Westerfield, M., Du, S.J., 2008. Sparc (Osteonectin) functions in morphogenesis of the pharyngeal skeleton and inner ear. Matrix Biol. 27, 561–572.
Sarmah, S., Barrallo-Gimeno, A., Melville, D.B., Topczewski, J., Solnica-Krezel, L., Knapik, E.W., 2010. Sec24D-dependent transport of extracellular matrix proteins is required for zebrafish skeletal morphogenesis. PLoS One 5, e10367.
Thisse, C., Thisse, B., 2008. High-resolution in situ hybridization to whole-mount zebrafish embryos. Nat. Protoc. 3, 59–69.
Walker, M.B., Kimmel, C.B., 2007. A two-color acid-free cartilage and bone stain for zebrafish larvae. Biotech. Histochem. 82, 23–28.
Walsh, E.C., Stainier, D.Y., 2001. UDP-glucose dehydrogenase required for cardiac valve formation in zebrafish. Science 293, 1670–1673.
Waterman, R.E., Bell, D.H., 1984. Epithelial fusion during early semicircular canal formation in the embryonic zebrafish, *Brachydanio rerio*. Anat. Rec. 210, 101–114.
Westerfield, M., 2007. The zebrafish book: a guide for the laboratory use of zebrafish (*Danio rerio*). University of Oregon Press, Eugene.
Whitfield, T.T., Granato, M., van Eeden, F.J., Schach, U., Brand, M., Furutani-Seiki, M., Haffter, P., Hammerschmidt, M., Heisenberg, C.P., Jiang, Y.J., et al., 1996. Mutations affecting development of the zebrafish inner ear and lateral line. Development 123, 241–254.